HHS Public Access

Author manuscript

Biomaterials. Author manuscript; available in PMC 2020 May 01.

Published in final edited form as:

Biomaterials. 2019 May ; 203: 52–62. doi:10.1016/j.biomaterials.2019.02.017.

HYDROGEL-BASED DELIVERY OF IL-10 IMPROVES TREATMENT OF BLEOMYCIN-INDUCED LUNG FIBROSIS IN MICE

Elya A. Shamskhou[1,**], **Michael J. Kratochvil**[2,3,**], **Mark E. Orcholski**[1], **Nadine Nagy**[3], **Gernot Kaber**[3], **Emily Steen**[4], **Swathi Balaji**[4], **Ke Yuan**[1], **Sundeep Keswani**[4], **Ben Danielson**[3], **Max Gao**[1], **Carlos Medina**[3], **Abinaya Nathan**[1], **Ananya Chakraborty**[1], **Paul L. Bollyky**[3,**], and **Vinicio A. De Jesus Perez**[1,**]

[1]Department of Medicine, Division of Pulmonary and Critical Care Medicine, Stanford University, Stanford, CA 94305

[2]Department of Materials Science and Engineering, Stanford University, Stanford, CA 94305

[3]Department of Medicine, Division of Infectious Disease, Stanford University, Stanford, CA 94305

[4]Department of Surgery, Division of Pediatric Surgery, Baylor College of Medicine and Texas Children's Hospital, Houston, TX 77030

Abstract

Idiopathic pulmonary fibrosis (IPF) is a life-threatening progressive lung disorder with limited therapeutic options. While interleukin-10 (IL-10) is a potent anti-inflammatory and anti-fibrotic cytokine, its utility in treating lung fibrosis has been limited by its short half-life. We describe an innovative hydrogel-based approach to deliver recombinant IL-10 to the lung for the prevention and reversal of pulmonary fibrosis in a mouse model of bleomycin-induced lung injury. Our studies show that a hyaluronan and heparin-based hydrogel system locally delivers IL-10 by capitalizing on the ability of heparin to reversibly bind IL-10 without bleeding or other complications. This formulation is significantly more effective than soluble IL-10 for both preventing and reducing collagen deposition in the lung parenchyma after 7 days of intratracheal administration. The antifibrotic effect of IL-10 in this system is dependent on suppression of TGF-β driven collagen production by lung fibroblasts and myofibroblasts. We conclude that hydrogel-based delivery of IL-10 to the lung is a promising therapy for fibrotic lung disorders.

* ydejesus@stanford.edu.

** Authors made equal primary contributions

Credit Author Statement

All authors were responsible for Conceptualization; Data curation; Formal analysis; Investigation; Methodology; Project administration; Resources; Software; Supervision; Validation; Visualization; Roles/Writing - original draft; Writing - review & editing.

Dr. Vinicio de Jesus Perez: Funding acquisition and other credits as above.

DECLARATIONS OF INTEREST: None

Keywords

Interleukin-10; Hyaluronic Acid; Fibrosis; Hydrogel; Drug Delivery; Idiopathic Pulmonary Fibrosis

INTRODUCTION

Idiopathic pulmonary fibrosis (IPF) is a rare but life-threatening condition with an incidence rate of 6.8–17.4 people per 100,000 per year in the USA [1]. IPF is characterized by progressive lung scarring that results in chronic respiratory failure, physical disability and severe hypoxemia [2–4]. The major histological feature of IPF is dense collagen accumulation produced by foci of highly proliferative fibroblasts (i.e. fibroblastic foci) [5, 6]. Current treatments for IPF include supplemental oxygen and antifibrotic agents such as nintedanib and pirfenidone, which can slow progression in patients with early disease [7–10]. Despite these therapies, the median survival for IPF patients remains poor (~2–3 years) and lung transplantation remains the treatment of choice for end-stage IPF [11]. Thus, there is an unmet need for novel anti-fibrotic therapies capable of slowing progression and improving clinical outcomes for IPF patients.

Interleukin-10 (IL-10) is a cytokine with potent anti-inflammatory and antifibrotic properties that makes it an appealing therapeutic candidate for IPF [12–17]. Long considered exclusively as an anti-inflammatory cytokine [18], IL-10 has also shown to possess anti-fibrotic effects as demonstrated by its capacity to suppress collagen I production in human skin fibroblasts [19]. Studies using lung tissue from IPF patients have shown significant elevation in IL-10 mRNA and protein levels, but whether this is reflective of a pathogenic or protective role is unclear [20]. Studies performed to date using the bleomycin mouse model of lung fibrosis have shown conflicting results as demonstrated by evidence that IL-10 could have either protective [15, 16, 21], null or even pro-fibrotic activity [22, 23]. One possible explanation for the discrepancy is that lung concentrations of IL-10 were not consistent between studies as a result of different methodologies and the very short half-life (1–2 minutes) of IL-10 in vivo [24]. The ideal approach would require steady release of IL-10 directly to lung tissue using a biocompatible vehicle with minimal toxicity to lung tissue. To this end, we have developed HH-10, a hydrogel generated from chemically-crosslinked hyaluronan and heparin designed to both retain moisture (hyaluronan) and to bind IL-10 (heparin).

Hydrogel-based release of IL-10 has previously been demonstrated, however, not in the context of delivery to lungs. A dock-and-lock peptide-polyethylene glycol hydrogel with erosion-based release of IL-10 was able to reduce renal inflammation and scarring in an animal model of chronic kidney disease[25]. In another report, a hyaluronic acid hydrogel, crosslinked via admantane-cyclodextrin host-guest complexes, was capable of controlled release of IL-10 with anti-transforming growth factor beta encapsulated in the gel. This hydrogel vehicle limited also limited fibrosis and inflammation in a chronic kidney disease animal model[26]. Using this same host-guest hyaluronic acid hydrogel, delivery of IL10 improved renal function and reduce inflammation in an ischemic acute kidney injury

model[27]. These systems showed release of IL-10 on the order of two to ten days. Dextran nanogels have also been used for release of IL-10. In a pair of reports, the Gama group characterized the dextran-IL-10 nanogels and showed release of active IL-10 in biological relevant amounts for 4 hours in vivo[28, 29]. Another report utilized intratracheal delivery for hydrogel-based therapies to administer basic Fibroblast Growth Factor to alleviate monocrotaline-induced pulmonary hypertension in rats[30].

To create HH-10, we used a commercially available hydrogel system (HyStem, ESI-Bio) that undergoes relatively rapid gelation kinetics via a thiol-ene reaction and is biologically safe for use. We chose a hyaluronic acid-heparin hydrogel system for these studies as both components (i) are naturally occurring extracellular matrix components, (ii) can be readily cleared by the body via enzymatic degradation, and (iii) are already used in various clinical treatments. Heparin is a known binding partner of IL-10, with an association constant of ~54 nM, thus providing a means for the IL-10 to remain sequestered in the hydrogel during the delivery process, and released in the hyaluronidase- and heparanase-rich fibrotic environment [31–33]. Similar approaches using heparin-immobilized protein drug payloads (e.g., growth factors) within hydrogels have been demonstrated to improve payload stability and drug efficacy [34, 35]. As a potential IPF therapy vehicle, hydrogels have been shown to be effective in several pulmonary conditions including hydrogel glues for lung air leaks, delivery of chemotherapeutic agents, and antibacterial hydrogels to prevent *Streptococcus pneumonia* colonization, among others [36–39]. We hypothesized that hydrogels loaded with IL-10 could be effectively delivered to the lungs of mice via a nasal route, and this material would have superior antifibrotic effects compared to PBS-dissolved IL-10.

In this study, we demonstrate that HH-10 can prevent and partially reverse fibrosis in mice treated with intratracheal bleomycin, a model that recapitulates many of the cardinal features of IPF such as scarring, excessive collagen deposition and fibroblast accumulation [40, 41]. Our studies show that HH-10 is superior in preventing and partially reversing lung fibrosis compared to IL-10 or HMW-HA alone. Taken together, our findings provide strong support for HH-10 as a novel therapeutic agent for the treatment of IPF.

METHODS AND MATERIALS

Reagents

The HyStem-HP Hydrogel kit using thiol-modified sodium hyaluronate with thiolmodified heparin (Heprasil-), thiol-modified gelatin (Gelin-S-), and polyethylene glycol diacrylate (PEGDA; Extralink-) was purchased from ESI-BIO. Thiol-modified sodium hyaluronate (Glycosil-) was purchased from ESI-BIO. Millicell cell culture inserts were purchased from Millipore-Sigma. Mouse IL-10 Quantikine enzyme-linked immunosorbent assay (ELISA) kits were purchased from R&D Systems. Bleomycin sulfate was purchased from MPBio (0219030610), reconstituted, and diluted based on manufacturer suggestion.

IPF human pulmonary fibroblast cells were obtained courtesy of Dr. Carol Feghali-Bostwick from the Medical University of South Carolina, Department of Rheumatology and Immunology. Healthy human pulmonary fibroblast cells were obtained from the following commercial sources: ScienCell (cat#3310)-lines HPF-a and HPF-c; Primary Cell Solutions

(cat#PCS-201–013)- Primary Lung Fibroblast Normal, Human. TGFβ-1 was purchased from Sigma (T7039), reconstituted, and diluted based on manufacturer suggestion. Fibroblast Media and supplements were purchased from ScienCell (2301) and used based on manufacturer protocol. Cells were used between passages 2–7 for experimental purposes. Wildtype C57Bl6J mice were purchased from Jackson Laboratories and received by the Stanford Veterinary Services Center. Sircol- soluble collagen assay was purchased from Biocolor Life Sciences Assay (S1000) and performed based on manufacturer protocol. EZ-Link Maleimide-PEG_2-Biotin was purchased from Thermo-Fischer Scientific (21901BID), reconstituted based on manufacturer protocol, and combined with HH at manufacturer protocol suggested concentration.

Antibodies

The following antibodies and reagents were used for paraffin embedded mouse lung tissues, as well as *in vitro* formalin fixed cell culture: F-Actin-488 conjugated (1:250 IF, A12379; Life Technologies Corporation); Collagen-1 (1:100 IF, 1:750 WB, NB600–408; Novus Biotechnologies); α-SMA (1:300 IHC, AB5694; Abcam); pSmad3 (1:400 IHC, 118825; Abcam); Hyaluronic Acid Binding Protein (1:100 IHC, 385911; Millipore); EZLink Maleimide-PEG_2-Biotin (21901BID; Thermo Scientific); Anti-Human IL-10 (1:200 IHC, ab9969;Abcam); STAT3 (1:500; Cell Signalling Technology, cat. #12640); Prolong Gold Antifade Solution containing DAPI (Life Technologies Corporation).

Whole Lung Lysate qPCR

Total cellular RNA was extracted from flash frozen healthy control and bleomycin mouse lung tissue using the RNeasy Mini Kit (Qiagen, Redwood City, CA) and converted to cDNA using the Fermentas Reverse Transcription Kit (Vilnius, Lithuania) following the manufacturer's protocol. Taqman primers for mouse GAPDH, HYAL1, HYAL2, HYAL3, and TMEM2 were purchased from Thermo Fischer Scientific. Mouse GAPDH was used for normalization. All real-time quantitative PCR studies were run in triplicates. The difference in mRNA expression was determined by delta CT against GAPDH, fold change determined compared to healthy control samples. N=4 for each group.

Hydrogel Preparation

The following solutions were prepared for *in vivo* treatments against bleomycin challenge: recombinant human IL-10 (diluted to 200 ng/mL, 573204, Biolegend) diluted in sterile phosphate buffered saline (PBS, 10 mM, pH 7.4); HH- 0.1% Heprasil (GS215, ESI Bio) solution from 1% stock diluted in sterile PBS, 4:1 in solution with Extralink (GS3007, ESI Bio) crosslinker; HH-10 (200 ng/mL IL-10 mixed with previously noted HH solution).

Hydrogel Tracking Experiment in vivo

Extracel and Extracel HP hydrogels (BioTime, Inc; Alameda, CA) were generated as per the manufacturer's instructions. In brief, a preparation of thiol-labeled HI and HA sold as "heprasil®" by BioTime, Inc. was resuspended in deionized water and mixed together with poly(ethyleneglycol) diacrylate (PEGDA) crosslinker (BioTime Inc.) at ratios per the manufacturer's instructions to achieve a 1% hydrogel. This material was made fresh

immediately prior to injection per the manufacturer's instructions for both *in vitro* and *in vivo* experiments. Unthiolated HA (1.5×10^6 Da) was purchased from Genzyme (Cambridge, MA). Growth factor reduced Matrigel matrix basal membrane (Corning; Bedford, MA) was diluted to a concentration of 7.5 mg/mL using MilliQ water (H_2O^{∞}, filtered to a resistance of 18.2 MΩ). All solutions were kept on ice throughout the preparation. Other reagents included type 1 collagen from rat tails (BD Biosciences, Franklin Lakes, NJ), Fibrinogen (Sigma Aldrich, St. Louis, MO) and recombinant IL-2 (Proleukin; Chiron Therapeutics, Emeryville, CA). Hydrogels of 50 μl volume incorporating an Alexa fluor 790 fluorescent tag (Thermo Fisher, Waltham, MA) were injected IP into the mice and allowed to polymerize *in situ*. Residual hydrogel mass was then assessed at 1, 5 and 12 days post injection using an IVIS 100 in vivo imaging system (Perkin Elmer, Waltham, MA).

Intranasal Instillation of Hydrogel in vivo

Mice were treated with hydrogel solutions, separate components, or PBS control via intranasal delivery at a volume of 50 μL per day for 7 days for treatment or prevention regimented cohorts under isoflurane anesthesia. Mice were placed in a flow-controlled isofluorane anesthesia chamber for roughly 2 minutes. A P100 micropipetter was loaded with 50 μL of the appropriate hydrogel component or control solution. Mice were removed from the anesthesia chamber and the solution was slowly pipetted drop by drop on their nostrils. The solution was continually pipetted drop by drop as they respired the solution into their airways and lungs, until all 50 μL had been administered. Mice were then returned to their original cage and monitored until awake. This process was continued for 7 continuous days in our prevention (starting 1 day after bleomycin administration) or treatment models (starting 7 days after bleomycin administration).

Hydrogel preparation for in vitro experiments

Heprasil, and Extralink solutions were prepared by dissolving the lyophilized solids in degassed water. These solutions were then combined into a 4:1 volume ratio of Heprasil:Extralink (100:25 μL) + 8 μL IL-10 (250 μg/mL) and 867 μL sterile PBS for 1mL of hydrogel total. These hydrogel combinations were then loaded onto a cell culture insert with 0.4 μm filter placed into 6-well plates with 350 μL per well of the 4:1 Heprasil combination (n=7). Gelation occurred within 20–30 minutes and all gels were transparent.

In vitro release kinetics of IL-10

To assess the ability of these hydrogel formulations to sustain the delivery of IL-10 and to study the release kinetics, IL-10 was noncovalently incorporated into the hydrogel combinations as above prior to crosslinking. The 350 μL of hydrogel (700 ng IL10 per gel) were then incubated in 1.3 mL of serum-free Dulbecco's modified eagle media (DMEM) chosen so as to meet the level of the filter and not submerge the gel. Media samples were collected in full every 24 hours for 7 days. After collection, fresh media was replaced in the same volume. IL-10 quantification in the collected media samples was then performed as per the commercial manufacturer's instructions (R&D Systems). The optical density (O.D.) of each sample was read at 450 nm on a spectrophotometric plate reader with 650 nm reference and blanked against a microwell containing DMEM alone. A four-parameter best-fit standard curve was derived with reference solutions of known IL-10 concentrations, and the

concentrations (ng/mL) of the media samples and controls were calculated from this curve. Concentration values for samples that had been diluted (day 1 samples were diluted 1:100; day 2 samples were diluted 1:10) were multiplied by the dilution factor.

Animals

All experimental protocols used in this study were approved by the Animal Care Committee at Stanford University (APLAC #26889) and adhered to the published guidelines of the National Institute of Health. Two to four-month old wildtype C57Bl6J mice were treated with PBS control or bleomycin (MPBio, 0219030610) at a concentration of 1500–2000 international units/kg weight intratracheally; mice were anesthetized via ketamine/xylazine cocktail (K113–10ML, Sigma). Twenty-four hours after bleomycin challenge, mice were intranasally treated with PBS control, IL-10, HH, or HH-10 (see “Hydrogel Preparation” for solution details) for 7 days starting the day after bleomycin challenge in prevention studies, or for 7 days starting 7 days after bleomycin challenge in treatment studies; mice were anesthetized for intranasal treatments via controlled isoflurane flow. Mice were checked daily throughout the duration of the experiment, including post-intranasal treatment gestation periods. After 21 days had elapsed post-bleomycin challenge, mice were euthanized using controlled isoflurane flow and cervical dislocation. Prior to dissection and tissue harvest, bronchoalveolar lavage (BAL) fluid was harvested from each mouse and immediately analyzed for cell counts. Animals were exsanguinated by perfusion through the right ventricle with 15–20 mL of PBS at 37 °C. Lung tissue was harvested and processed for paraffin embedding and Sircol- assay. Tissues were paraffin embedded and stained for trichrome and hematoxylin/eosin.

Sircol- Assay ex vivo

Lung collagen content from experimental mice was determined via the Sircol- Soluble Collagen Assay (Biocolor Life Science Assays, S1000; Carrickfergus, County Antrim, UK). Once lung tissue was harvested post-perfusion, lungs were then chopped and homogenized, and the assay was performed following the manufacturer protocol.

Biotin Functionalization of HH

To visualize the location of exogenous hyaluronan and the site of treatment deposition, HH was functionalized with biotin by adding 20 mM EZ-Link Maleimide-PEG_2-Biotin (21901BID; Thermo Scientific) to HH as per the manufacturer’s protocol. HH was prepared in the same manner as prevention and treatment arms of this study (0.1% Heprasil solution from 1% stock diluted in sterile PBS), with reconstituted EZ-Link Maleimide-PEG_2-Biotin added to this solution at a dilution based on manufacturer protocol. This solution was allowed to react and form for 1–4 hours at room temperature with shaking, followed by storage in 4°C until time of intranasal deposition. Deposition occurred during days 1–7 post-bleomycin or PBS challenge; mice were sacrificed, and tissues were harvested at 21 days. Deposited Maleimide-PEG_2-Biotin conjugated hydrogel was visualized via biotin-streptavidin linkage conjugated to a 488 fluorophore.

HA ELISA

We used a previously described method to quantify HA in tissues[42]. In brief, tissues were lyophilized and weighed, followed by digestion with proteinase K (250 μg/ml) in 100 mM ammonium acetate, pH 7.0, overnight at 60°C. After digestion, the enzyme was inactivated by heating to 100°C for 20 minutes. The total amount of HA was determined by a modified competitive ELISA in which the samples to be assayed were first mixed with biotinylated HA-binding protein and then added to HA-coated microtiter plates. The final signal was inversely proportional to the level of hyaluronan added to the biotinylated proteoglycan.

HA staining

We used a previously described method to stain for HA in tissues[43]. After deparaffinization, endogenous peroxidases were blocked using H_2O_2 in methanol. Tissue sections were rehydrated in a series of graded ethanol. Rehydrated tissue sections were blocked in 1% bovine serum albumin (BSA) in PBS for 1 hour at room temperature and incubated overnight at 4°C with biotinylated hyaluronan binding protein (4 μg/ml). After two PBS washes, the tissue sections were incubated with the Vector “Elite” ABC-HP kit (Vector Labs; Burlingame, CA) in a moist chamber for 30 minutes at room temperature. Detection was performed using the Vector NovaRed substrate (Vector Labs) for 10 minutes at room temperature. The sections were counterstained with hematoxylin.

Immunofluorescence and Immunohistochemistry Staining

Cell Culture: For healthy and IPF human fibroblast cell culture staining, the following steps were performed: once the experiment had concluded, cells were washed with PBS three times followed by fixation by 4% paraformaldehyde for 10–15 minutes. Following fixation, cells were then permeabilized with PBS containing 0.1% Triton X-100 (PBST) and blocked with normal goat serum for 1 hour at room temperature, followed by primary antibody incubation overnight at 4°C. Th e next day, cells were washed again with PBST and incubated with 488, 594, or 647 fluorophore containing secondary antibodies for 1 hour at room temperature (Life Technologies Corporation). Slides were mounted with Prolong Gold Antifade Solution containing DAPI (Life Technologies Corporation).

Immunohistochemistry Staining- Mouse Tissue: For mouse lung tissues, sections were sourced from paraffin-embedded tissues. Standard deparaffinization techniques were used for paraffin-embedded tissues sections with antigen retrieval via citrate buffer. Following deparaffinization, slides were prepared by washing in PBST and endogenous peroxidases were quenched via 0.3% hydrogen peroxide solution for 30 minutes. Following quenching, slides were washed in PBST and blocked in diluted normal goat serum for 20 minutes at room temperature, followed by primary antibody incubation overnight at 4 °C. The next day, slides were washed with PBST three times for five minutes each and incubated with the Vector “Elite” ABC-HP kit (Vector Labs; Burlingame, CA) in a moist chamber for 45 minutes at room temperature for both the HRP-conjugated secondary reagent and ABC reagent with washes with PBST in between each incubation. Detection was performed using the Stable DAB reagent (Invitrogen, 750118) for 10 minutes at room temperature. The

sections were counterstained with hematoxylin. The Ashcroft score was used to classify the severity of fibrosis in trichrome-stained lung sections [44].

Immunofluorescence for STAT3 detection in human pulmonary fibroblasts: Human pulmonary fibroblast cells (1.5×10^4 cells per chamber) were seeded into two 4-chamber culture slides (Lab-Tek) and allowed to attach. The cells were treated with DMEM elution media obtained from day 1 (35 ng/mL; n=2) and day 2 (26 ng/mL; n=2) of incubation with HH-10. DMEM spiked with recombinant IL-10 matching the average IL10 concentration in the day 1 eluate (30 ng/mL, n=2) was used as positive control, while DMEM alone was used as negative control (n=2). All incubations were carried out for 1 h followed by rinsing with 1XPBS and fixation with 2% paraformaldehyde for 10 min at room temperature. After washing with PBS three times for three minutes each, the cells were permeabilized with lyophilized bovine serum albumin dissolved in 10% normal goat serum in PBS plus 1% saponin solution. The cells were then incubated with anti-STAT3 monoclonal rabbit antibody (1:500; Cell Signaling Technology, cat. #12640) diluted in 1% saponin solution plus 0.1% Triton X-100 for 2 h at room temperature. After washing with buffer solution three times for 3 min each, the cells were co-incubated with a Texas Red-labeled goat anti-rabbit secondary antibody (1:1000; Thermo-Fisher Scientific) and with phalloidin-iFluor 488 probe (1:1000; Abcam) diluted in 1% saponin and 0.1% Triton X-100 for 1 h at room temperature. After washing with buffer solution three times for 3 min each, the slides were mounted with DAPI and coverslipped. The cells were examined by fluorescence microscopy (Leica DMi8 with Leica application Suite X version 3.0.4.16319).

Statistical Analysis

The number of samples or animals studied per experiment is indicated in the figure legends. Values from multiple experiments are expressed as mean +/− SEM. Statistical significance was determined using unpaired t-tests or one-way ANOVA followed by Dunnett's or Bonferroni's multiple comparison tests unless stated otherwise. A value of $P<0.05$ was considered significant.

RESULTS AND DISCUSSION

IL-10 Decreases Fibrotic Markers in Healthy and IPF Pulmonary Lung Fibroblasts Activated by Recombinant TGFβ-1

We first investigated whether treatment with IL-10 could antagonized the pro-fibrotic effects of TGFβ-1 in human pulmonary fibroblast cells collected from healthy individuals and individuals with IPF. TGFβ-1 is a well-established pro-fibrotic cytokine that is upregulated in IPF. When exposed to TGFβ-1, fibroblasts increase collagen-I production and augment expression of f-actin, a marker of myofibroblast transformation [45].

At baseline, unstimulated healthy lung fibroblasts showed minimal collagen and f-actin expression but treatment with TGFβ-1 for 24 hours led to a substantial increase in cytoplasmic collagen-I and f-actin (Fig. 1A, **upper panels**). However, cells costimulated with IL-10 displayed significantly less collagen-I and f-actin in response to TGFβ-1 (Fig. 1B and C). Compared to healthy cells, human IPF fibroblasts exhibited a trend towards higher

collagen and f-actin expression at baseline as well as a modest increase upon TGFβ-1 stimulation that did not achieve statistical significance (Fig. 1A, **lower panels**). Stimulation with IL-10 alone or IL-10 in combination with TGFβ−1 significantly attenuated collagen-I expression while f-actin expression did not decrease significantly (Fig. 1B and C). Taken together, our findings indicate that IL-10 can reduce TGFβ-1 mediated collagen I production by both healthy and IPF lung fibroblasts but its capacity to reduce myofibroblast differentiation is limited to healthy lung fibroblasts.

Quantification of IL-10 Release Kinetics from Hyaluronan and Heparin (HH) Hydrogels

Prior to our in vivo studies, we evaluated the binding capacity of HH hydrogels loaded with recombinant IL-10. We generated a 0.1% hydrogel comprised of thiolated hyaluronan and thiolated heparin initially dissolved in an IL-10 solution and crosslinked with PEGDA. We performed daily, serial washes of IL-10-loaded HH gels to examine the rate at which IL-10 was released from the gels incubated at physiological conditions in the absence of enzymes. We observed that 350 μL of HH-10 gels (loaded with 700 ng of IL-10) released ~39 ng of IL-10 (~5.6% of the total amount loaded) in the first 24 h when incubated in DMEM at 37 °C, with only ~3 ng of IL-10 released in the following 72 h (Fig. 2A). Over the course of six days, approximately 6% of the total loaded IL-10 was released from the HH hydrogels. Indeed, this data suggests that ~94% of the loaded IL-10 remains immobilized within the HH hydrogel and would likely require the presence of hyaluronidases and heparinases *in vivo* to be released into the surrounding lung parenchyma. This immobilized state may serve as protection for the IL-10 payload until the point of enzymatic release into the fibrotic lung environment.

IL-10 Released by HH-10 Activates STAT3 Signaling in Human Pulmonary Fibroblasts

The fibroblast is considered the “effector” cell in the pathogenesis of fibrosis through production of collagen and other ECM components[46, 47]. Our group and others have previously reported that IL-10 suppresses the pro-fibrotic behavior of dermal fibroblasts through activation and nuclear translocation of STAT3, a transcription factor that suppresses expression of pro-fibrotic and pro-inflammatory genes[48–50]. To determine whether the IL-10 eluted from HH-10 activates STAT3, we exposed human pulmonary fibroblasts to DMEM incubated with HH-10 for 1 and 2 days (i.e. “elution media”) and compared against DMEM spiked with recombinant IL-10 at concentrations matching those of day 1 elution media (see Methods). Compared to unstimulated fibroblasts (Supp. Fig. 1A), both Day 1 and 2 elution media triggered relocation of STAT3 to fibroblast nuclei (Supp. Fig. 1B and C). The STAT3 nuclear relocation was comparable to that seen in cells stimulated with IL-10 spiked media (Supp. Fig. 1D). Taken together, these findings demonstrate that IL-10 effectively elutes from the hydrogel at concentrations that are capable of triggering STAT3 nuclear relocation, a marker of signaling activation, as indicated by comparison with the spiked media.

HH-10 is Superior to HH or IL-10 in Preventing Bleomycin-Induced Lung Fibrosis

Following the *in vitro* studies, we tested whether HH-10 could ameliorate lung fibrosis in the murine bleomycin fibrosis model. In this model, intratracheal challenge of bleomycin results

in scarred lung tissue in the major airways over a period of ~1–2 weeks, usually leading to death in ~2–4 weeks (Supp. Fig. 2A and B). We used this model to test our hypothesis that IL-10 delivered via hydrogel would prevent the development of lung fibrosis after bleomycin injury. All interventions were conducted intranasally, where a sedated mouse would aspirate either the hydrogel, or PBS solutions through the nostrils. Prior to starting the studies, we documented that IL-10 in the lung of healthy mice was found predominantly in airway epithelial cells with a more diffuse signal seen in the parenchyma (Supp. Fig. 3).

To document that nasal aspiration resulted in effective delivery of HH-10 to distal airways and lung parenchyma, an HH-formulation modified with a biotin-PEG linkage was administered to mice once a day for 7 days after bleomycin or PBS challenge (Supp. Fig. 5A). This modified HH formulation was visualized in lung tissue via fluorescence microscopy by treating the excised lung tissue with fluorescently conjugated streptavidin. Indeed, significant deposition of the hydrogel was observed in bronchioli and parenchyma of healthy (Fig. 2B) and bleomycin-challenged mice (Fig. 2C). Additional images demonstrated hydrogel deposition in major airways and distal portions of the lung (Supp. Fig. 4A and B). Importantly, all mice tolerated the hydrogel deposition well and no delivery-related mortality was observed.

To better understand the degradation of HH-10 in the lung, hyaluronidase 1–3 and TMEM2 (also known as cell migration inducing hyaluronidase 2) expression patterns were measured in healthy and bleomycin mouse lung lysates. Tissues were homogenized for RNA extraction and patterns showed increased expression of HYAL1, HYAL2, and TMEM2 in fibrotic tissues (Supp. Fig. 4C). This data suggests that injured tissue increases the presence of enzymes that breakdown hyaluronan, potentially leading to enhanced release of the hydrogel-bound IL-10.

The therapeutic efficacy and safety of HH-10 was first evaluated in a bleomycin prevention model (i.e. inflammatory phase of bleomycin lung injury prior to appearance of fibrosis). In these prevention experiments, intervention in bleomycin-challenged mice was done with a PBS control, IL-10 (200 ng/mL), HH (0.1% solution with 0.025% crosslinker), or HH-10 (combination of 200 ng/ml IL-10 in a gel of HH 0.1% solution with 0.025% crosslinker) administered daily over the course of 7 days beginning one day after bleomycin administration. After the final treatment, mice were monitored for an additional 14 days for a total of 21 days following initial bleomycin administration (Fig. 3A). Whereas mice treated in the PBS control group suffered a 25% mortality rate, survival was significantly improved in mice treated with HH, IL-10 alone, or HH-10 (Supp. Fig. 2A). After 21 days, the surviving mice were sacrificed, and lungs were harvested for histology and biochemical analysis. The lungs of bleomycin exposed mice treated with PBS (i.e. negative control) exhibited large collagen-rich lesions (Fig. 3B, **upper panels**) with abundant α-SMA expressing myofibroblasts (Fig. 3B, **lower panels**). While the lungs from mice treated with either IL-10 or HH alone also displayed discrete bleomycin induced fibrosis, collagen-rich lesions were smaller (Fig. 3B, **upper middle two panels**) with fewer α-SMA expressing myofibroblasts (Fig. 3B, **lower middle two panels**). To our surprise, mice treated with HH-10 had significantly preserved lung architecture, as evidenced by minimal fibrosis (Fig.

3B, **upper right panel**) and α-SMA staining predominantly from smooth muscle cells around airways and blood vessels (Fig. 3B, **lower right panel**).

Next, we compared total collagen content in whole lung tissue from all experimental groups using the Sircol- assay, a dye-based quantitative method to measure soluble extracellular collagen. Compared to PBS treated mice, lung tissue from mice treated with IL-10 or HH alone demonstrated a modest but significant decrease in total collagen content (Fig. 3C). Consistent with our histological findings, HH-10-treated lungs demonstrated a substantial decrease in collagen content that was comparable to that found in healthy (non-bleomycin) lungs (Fig. 3C). In agreement with these findings, Ashcroft scores of HH-10 treated lungs were significantly lower compared to PBS, IL-10 or HH alone, which suggest the fibrosis was attenuated by the HH-10 intervention (Fig. 3D). Finally, we quantified the cellular content in BAL samples obtained prior to lung removal. As anticipated, we found that PBS-treated mice had a significantly higher BAL cell count than healthy animals; however, BAL cell counts from mice treated with IL-10, HH, and HH-10 were comparable to those from healthy animals (Fig. 3E). Taken as a whole, these data indicate that HH-10 is superior to IL-10 or HH alone in preventing bleomycin-induced fibrosis.

HH-10 Reduces Fibrosis Burden in Mice with Established Lung Fibrosis

We next examined whether interventions given 7 days after bleomycin challenge can reverse established lung fibrosis. This experimental model is analogous to the middle and late phases of IPF most commonly seen in clinical settings [51]. From day 8 to day 14, mice were treated intranasally with either PBS, IL-10, HH, or HH-10 daily for seven days (Fig. 4A). At the end of 21 days following bleomycin administration, the animals were sacrificed for downstream analysis as previously described.

In this experimental setting, survival rates were highest in the IL-10 treatment group followed by the HH-10 and HH groups (Supp. Fig. 2B). While we have no definite explanation for this, we speculate that the higher viscosity of hydrogels could have worsened respiratory mechanics in these mice by plugging small airways. This increased survival in the IL-10 group did not correlate to better lung histology or tissue outcomes. Compared to PBS treated mice (Fig. 4B, **left panels**), lung trichrome stain and IHC of all treatment groups showed a mild reduction in size of fibrotic lesions and αSMA content (Fig. 4B, **middle panels**), with HH-10 treated mice demonstrating the least severity (Fig. 4B, **right panel**). While we found no significant differences in total collagen content across groups (Fig. 4C), Ashcroft scores were significantly lower in IL-10 and HH-10 treated mice (Fig. 4D). On the other hand, BAL cell content was significantly reduced only in HH and HH-10 lungs after 21 days of bleomycin administration (Fig. 4E). Taken together, our treatment data demonstrates that HH-10 can attenuate established fibrosis although this effect has lesser magnitude compared to prevention studies (Fig. 3).

Lung Hyaluronan Content is Unaffected by HH-10 Treatment

An important aspect of translating HH-10 into a viable clinical therapy is safety with chronic use. One major concern is that chronic use of HH-10 could result in irreversible hyaluronan accumulation into the lung, an event which could potentially lead to long-term adverse

consequences, such as paradoxical exacerbation of IPF [52]. To address this, we measured hyaluronan (HA) in lung tissues and BAL samples obtained at 21 days. Similar to previous reports, HA was found in high density within the fibrotic lesions of PBS treated groups; however, lungs from all treatment groups demonstrated significantly less HA, especially in areas surrounding fibrotic lesions [53] (Supp. Fig. 5A). In our assessment, none of the different treatment arms showed any observable qualitative difference in HA accumulation across healthy tissue. Similarly, an HA ELISA performed in available flash frozen lung tissues (Supp. Fig. 5B) and BAL fluid (Supp. Fig. 5C) revealed that HA content was nearly the same across all groups, including the PBS treated cohort.

Taken together, our findings indicate that treatment with HH and HH-10 do not result in HA accumulation in the lung tissue, likely due to catabolism of HA by endogenous hyaluronidases and subsequent cellular uptake and clearance.

Smad3 Phosphorylation, a Marker of TGFβ-1 Activity, is Decreased in HH-10 Treated Mice

A major driver of fibrosis in IPF and bleomycin models of lung fibrosis is the TGFβ-1 signaling pathway [54, 55]. A member of the TGF signaling superfamily, TGFβ-1 signals through surface receptors that phosphorylate (i.e. activate) Smad2/3, a cytoplasmic protein that, upon phosphorylation, translocates to the nucleus and upregulates collagen and SMA production in fibroblasts [56, 57]. IHC for phospho (p) Smad3 in lung sections from the prevention studies (Fig. 5A, **upper panels**) demonstrated significant reduction in nuclear pSmad3 only in HH-10 treated mice (Fig. 5B). However, in the treatment study (Fig. 5A, **lower panels**), we found significant reductions in nuclear pSmad3 in the lungs of IL-10 and HH-10 treated animals, which were significantly greater in the latter (Fig. 5C). Lower magnifications images of these areas can be found in Supp. Fig. 6.

In summary, both IL-10 and HH-10 antagonize TGFβ-1 activation *in vivo.* These findings support the observations from our earlier *in vitro* studies with IL-10 (**see** Fig. 1) and provide a mechanistic rationale for the salutary effects observed with HH-10.

CONCLUSIONS

We demonstrate that a hydrogel delivery system for IL-10 attenuates lung fibrosis in an animal model of IPF in a superior fashion than treatment with either IL-10 or HH alone. We also demonstrate that intranasal administration can effectively deliver sufficient hydrogel deposition to the small airways and lung parenchyma. Furthermore, we demonstrate that IL-10 decreases fibrosis due to inhibition of TGFβ-1 activation of fibroblasts from IPF patients. Reduction of Smad3 phosphorylation is key to the action of IL-10 on the human fibroblasts. Strikingly, Smad3 phosphorylation was demonstrated to be significantly down-regulated in the HH-10-treated mice, thus suggesting the same mechanism of treatment highlighted in human IPF cells was active in the *in vivo* testing.

There are several limitations to this study. While it is tempting to propose that much of the fibrosis seen in the bleomycin model and IPF is driven by fibroblasts, we must stress that both IL-10 and the utilized hydrogel also have potent anti-inflammatory effects and the capacity to upregulate metalloproteinases which could also contribute to reduction of

fibrosis. Also, we acknowledge that the pathobiology of IPF involves other cell types (e.g., alveolar cells, macrophages, lymphocytes) whose biological response to these molecules should be studied to understand how HH-10 modulates lung fibrosis.

In conclusion, we propose that our HH-10 formulation is an effective method to deliver therapeutic amounts of IL-10 directly to the lung via inhalation. We believe that HH-10 could be applied to management of IPF alone or in combination with available therapies resulting in preservation of pulmonary function and improved outcomes. Most importantly, the implications of our work are not limited to IPF, but likely offer broad applications in other lung diseases that are also characterized by excessive fibroplasia (e.g. scleroderma, radiation induced fibrosis).

Supplementary Material

Refer to Web version on PubMed Central for supplementary material.

ACKNOWLEDGEMENTS

We would like to acknowledge the hard work and help of Abinaya Nathan and Ananya Chakraborty for graphical representation and statistical analysis of data presented in this manuscript.

FUNDING SOURCES

This work was supported by a Pulmonary Fibrosis Foundation IM Rosenzweig Award, NIH R01 HL134776, R01 HL134776-02, R03 HL133423-01, AHA Beginning Grant in Aid, a Stanford Cardiovascular Institute (CVI) and Translational Research and Applied Medicine (TRAM) to V. de Jesus Perez. K. Yuan was supported by American Heart Association Scientist Development Grant (15SDG25710448), the Parker B. Francis Fellowship, and the Pulmonary Hypertension Association Proof of Concept Award. M.J.K. was supported by the Stanford ChEM-H Interdisciplinary Postdoctoral Training Program in Quantitative Mechanobiology.

REFERENCES

1. Nalysnyk L, et al., Incidence and prevalence of idiopathic pulmonary fibrosis: review of the literature. Eur Respir Rev, 2012 21(126): p. 355–61. [PubMed: 23204124]
2. Kekevian A, Gershwin ME, and Chang C, Diagnosis and classification of idiopathic pulmonary fibrosis. Autoimmun Rev, 2014 13(4–5): p. 508–12. [PubMed: 24424167]
3. Kendall RT and Feghali-Bostwick CA, Fibroblasts in fibrosis: novel roles and mediators. Front Pharmacol, 2014 5: p. 123. [PubMed: 24904424]
4. Woodcock HV and Maher TM, The treatment of idiopathic pulmonary fibrosis. F1000Prime Rep, 2014 6: p. 16. [PubMed: 24669297]
5. Bagnato G and Harari S, Cellular interactions in the pathogenesis of interstitial lung diseases. Eur Respir Rev, 2015 24(135): p. 102–14. [PubMed: 25726561]
6. Huang SK and Horowitz JC, Outstaying their Welcome: The Persistent Myofibroblast in IPF. Austin J Pulm Respir Med, 2014 1(1): p. 3. [PubMed: 25309962]
7. Bonella F, Stowasser S, and Wollin L, Idiopathic pulmonary fibrosis: current treatment options and critical appraisal of nintedanib. Drug Des Devel Ther, 2015 9: p. 6407–19.
8. Huang J, et al., Nintedanib inhibits fibroblast activation and ameliorates fibrosis in preclinical models of systemic sclerosis. Ann Rheum Dis, 2016 75(5): p. 883–90. [PubMed: 25858641]
9. Wollin L, et al., Mode of action of nintedanib in the treatment of idiopathic pulmonary fibrosis. Eur Respir J, 2015 45(5): p. 1434–45. [PubMed: 25745043]
10. Adamali HI and Maher TM, Current and novel drug therapies for idiopathic pulmonary fibrosis. Drug Des Devel Ther, 2012 6: p. 261–72.

11. Kumar A, et al., Lung transplantation in idiopathic pulmonary fibrosis. Expert Rev Respir Med, 2018 12(5): p. 375–385. [PubMed: 29621919]
12. Martinez JA, et al., Increased expression of the interleukin-10 gene by alveolar macrophages in interstitial lung disease. Am J Physiol, 1997 273(3 Pt 1): p. L676–83. [PubMed: 9316504]
13. Zgheib C, Xu J, and Liechty KW, Targeting Inflammatory Cytokines and Extracellular Matrix Composition to Promote Wound Regeneration. Adv Wound Care (New Rochelle), 2014 3(4): p. 344–355. [PubMed: 24757589]
14. Peranteau WH, et al., IL-10 overexpression decreases inflammatory mediators and promotes regenerative healing in an adult model of scar formation. J Invest Dermatol, 2008 128(7): p. 1852–60. [PubMed: 18200061]
15. Nakagome K, et al., In vivo IL-10 gene delivery attenuates bleomycin induced pulmonary fibrosis by inhibiting the production and activation of TGF-beta in the lung. Thorax, 2006 61(10): p. 886–94. [PubMed: 16809410]
16. Arai T, et al., Introduction of the interleukin-10 gene into mice inhibited bleomycin-induced lung injury in vivo. Am J Physiol Lung Cell Mol Physiol, 2000 278(5): p. L914–22. [PubMed: 10781421]
17. Yamamoto T, Eckes B, and Krieg T, Effect of interleukin-10 on the gene expression of type I collagen, fibronectin, and decorin in human skin fibroblasts: differential regulation by transforming growth factor-beta and monocyte chemoattractant protein-1. Biochem Biophys Res Commun, 2001 281(1): p. 200–5. [PubMed: 11178980]
18. Moore KW, et al., Interleukin-10. Annu Rev Immunol, 1993 11: p. 165–90. [PubMed: 8386517]
19. Reitamo S, et al., Interleukin-10 modulates type I collagen and matrix metalloprotease gene expression in cultured human skin fibroblasts. J Clin Invest, 1994 94(6): p. 2489–92. [PubMed: 7989607]
20. Bergeron A, et al., Cytokine profiles in idiopathic pulmonary fibrosis suggest an important role for TGF-beta and IL-10. Eur Respir J, 2003 22(1): p. 69–76. [PubMed: 12882453]
21. Garcia-Prieto E, et al., Resistance to bleomycin-induced lung fibrosis in MMP-8 deficient mice is mediated by interleukin-10. PLoS One, 2010 5(10): p. e13242. [PubMed: 20949050]
22. Barbarin V, et al., Pulmonary overexpression of IL-10 augments lung fibrosis and Th2 responses induced by silica particles. Am J Physiol Lung Cell Mol Physiol, 2005 288(5): p. L841–8. [PubMed: 15608148]
23. Li Y, et al., Severe lung fibrosis requires an invasive fibroblast phenotype regulated by hyaluronan and CD44. J Exp Med, 2011 208(7): p. 1459–71. [PubMed: 21708929]
24. Le T, et al., Regulation of interleukin-10 gene expression: possible mechanisms accounting for its upregulation and for maturational differences in its expression by blood mononuclear cells. Blood, 1997 89(11): p. 4112–9. [PubMed: 9166853]
25. Soranno DE, et al., Immunotherapy with injectable hydrogels to treat obstructive nephropathy. J Biomed Mater Res A, 2014 102(7): p. 2173–80. [PubMed: 23913854]
26. Rodell CB, et al., Local immunotherapy via delivery of interleukin-10 and transforming growth factor beta antagonist for treatment of chronic kidney disease. J Control Release, 2015 206: p. 131–9. [PubMed: 25804871]
27. Soranno DE, et al., Delivery of interleukin-10 via injectable hydrogels improves renal outcomes and reduces systemic inflammation following ischemic acute kidney injury in mice. Am J Physiol Renal Physiol, 2016 311(2): p. F362–72. [PubMed: 26962109]
28. Carvalho V, et al., Self-assembled dextrin nanogel as protein carrier: controlled release and biological activity of IL-10. Biotechnol Bioeng, 2011 108(8): p. 1977–86. [PubMed: 21391205]
29. Carvalho V, et al., Biological activity of heterologous murine interleukin-10 and preliminary studies on the use of a dextrin nanogel as a delivery system. Int J Pharm, 2010 400(1–2): p. 234–42. [PubMed: 20816730]
30. Hirose K, et al., Novel approach with intratracheal administration of microgelatin hydrogel microspheres incorporating basic fibroblast growth factor for rescue of rats with monocrotal-ineinduced pulmonary hypertension. J Thorac Cardiovasc Surg, 2008 136(5): p. 1250–6. [PubMed: 19026811]

31. He L, et al., HMGB1 exacerbates bronchiolitis obliterans syndrome via RAGE/NF-kappaB/HPSE signaling to enhance latent TGF-beta release from ECM. Am J Transl Res, 2016 8(5): p. 1971–84. [PubMed: 27347307]
32. Nadir Y, et al., Heparanase procoagulant activity is elevated and predicts survival in non-small cell lung cancer patients. Thrombosis Research, 2014 134(3): p. 639–642. [PubMed: 25065557]
33. Monzón ME, et al., Hyaluronidase Expression and Activity Is Regulated by Pro-Inflammatory Cytokines in Human Airway Epithelial Cells. American Journal of Respiratory Cell and Molecular Biology, 2008 39(3): p. 289–295. [PubMed: 18390475]
34. Sakiyama-Elbert SE and Hubbell JA, Development of fibrin derivatives for controlled release of heparin-binding growth factors. Journal of Controlled Release, 2000 65(3): p. 389–402. [PubMed: 10699297]
35. Sakiyama-Elbert SE, Incorporation of heparin into biomaterials. Acta Biomaterialia, 2014 10(4): p. 1581–1587. [PubMed: 24021232]
36. Xu K, et al., Cold Chain-Free Storable Hydrogel for Infant-Friendly Oral Delivery of Amoxicillin for the Treatment of Pneumococcal Pneumonia. ACS Appl Mater Interfaces, 2017 9(22): p. 18440–18449. [PubMed: 28513136]
37. Mangal S, et al., Pulmonary delivery of nanoparticle chemotherapy for the treatment of lung cancers: challenges and opportunities. Acta Pharmacol Sin, 2017 38(6): p. 782–797. [PubMed: 28504252]
38. Hu C, et al., Regulating cancer associated fibroblasts with losartan-loaded injectable peptide hydrogel to potentiate chemotherapy in inhibiting growth and lung metastasis of triple negative breast cancer. Biomaterials, 2017 144: p. 60–72. [PubMed: 28823844]
39. Fuller C, Reduction of intraoperative air leaks with Progel in pulmonary resection: a comprehensive review. J Cardiothorac Surg, 2013 8: p. 90. [PubMed: 23590942]
40. Izbicki G, et al., Time course of bleomycin-induced lung fibrosis. Int J Exp Pathol, 2002 83(3): p. 111–9. [PubMed: 12383190]
41. Zhang HY, et al., Lung fibroblast alpha-smooth muscle actin expression and contractile phenotype in bleomycin-induced pulmonary fibrosis. Am J Pathol, 1996 148(2): p. 527–37. [PubMed: 8579115]
42. Underhill CB, et al., CD44 positive macrophages take up hyaluronan during lung development. Dev Biol, 1993 155(2): p. 324–36. [PubMed: 8432391]
43. Evanko SP, et al., Proteoglycan distribution in lesions of atherosclerosis depends on lesion severity, structural characteristics, and the proximity of platelet-derived growth factor and transforming growth factor-beta. Am J Pathol, 1998 152(2): p. 533–46. [PubMed: 9466580]
44. Ashcroft T, Simpson JM, and Timbrell V, Simple method of estimating severity of pulmonary fibrosis on a numerical scale. J Clin Pathol, 1988 41(4): p. 467–70. [PubMed: 3366935]
45. Raghu G, et al., Collagen synthesis by normal and fibrotic human lung fibroblasts and the effect of transforming growth factor-beta. Am Rev Respir Dis, 1989 140(1): p. 95–100. [PubMed: 2751176]
46. Pardo A and Selman M, Lung Fibroblasts, Aging, and Idiopathic Pulmonary Fibrosis. Ann Am Thorac Soc, 2016 13 Suppl 5: p. S417–S421. [PubMed: 28005427]
47. Wynn TA, Cellular and molecular mechanisms of fibrosis. J Pathol, 2008 214(2): p. 199–210. [PubMed: 18161745]
48. Sziksz E, et al., Fibrosis Related Inflammatory Mediators: Role of the IL-10 Cytokine Family. Mediators Inflamm, 2015 2015: p. 764641. [PubMed: 26199463]
49. Balaji S, et al., Interleukin-10-mediated regenerative postnatal tissue repair is dependent on regulation of hyaluronan metabolism via fibroblast-specific STAT3 signaling. FASEB J, 2017 31(3): p. 868–881. [PubMed: 27903619]
50. Shi J, et al., Anti-fibrotic actions of interleukin-10 against hypertrophic scarring by activation of PI3K/AKT and STAT3 signaling pathways in scar-forming fibroblasts. PLoS One, 2014 9(5): p. e98228. [PubMed: 24878845]
51. Raghu G, et al., An official ATS/ERS/JRS/ALAT statement: idiopathic pulmonary fibrosis: evidence-based guidelines for diagnosis and management. Am J Respir Crit Care Med, 2011 183(6): p. 788–824. [PubMed: 21471066]

52. Jiang D, Liang J, and Noble PW, Hyaluronan in tissue injury and repair. Annu Rev Cell Dev Biol, 2007 23: p. 435–61. [PubMed: 17506690]

53. Albeiroti S, Soroosh A, and de la Motte CA, Hyaluronan's Role in Fibrosis: A Pathogenic Factor or a Passive Player? Biomed Res Int, 2015. 2015: p. 790203.

54. Sporn MB, et al., Transforming growth factor-beta: biological function and chemical structure. Science, 1986 233(4763): p. 532–4. [PubMed: 3487831]

55. Varga J, Rosenbloom J, and Jimenez SA, Transforming growth factor beta (TGF beta) causes a persistent increase in steady-state amounts of type I and type III collagen and fibronectin mRNAs in normal human dermal fibroblasts. Biochem J, 1987 247(3): p. 597–604. [PubMed: 3501287]

56. Roberts AB, TGF-beta signaling from receptors to the nucleus. Microbes Infect, 1999 1(15): p. 1265–73. [PubMed: 10611754]

57. Massague J and Wotton D, Transcriptional control by the TGF-beta/Smad signaling system. EMBO J, 2000 19(8): p. 1745–54. [PubMed: 10775259]

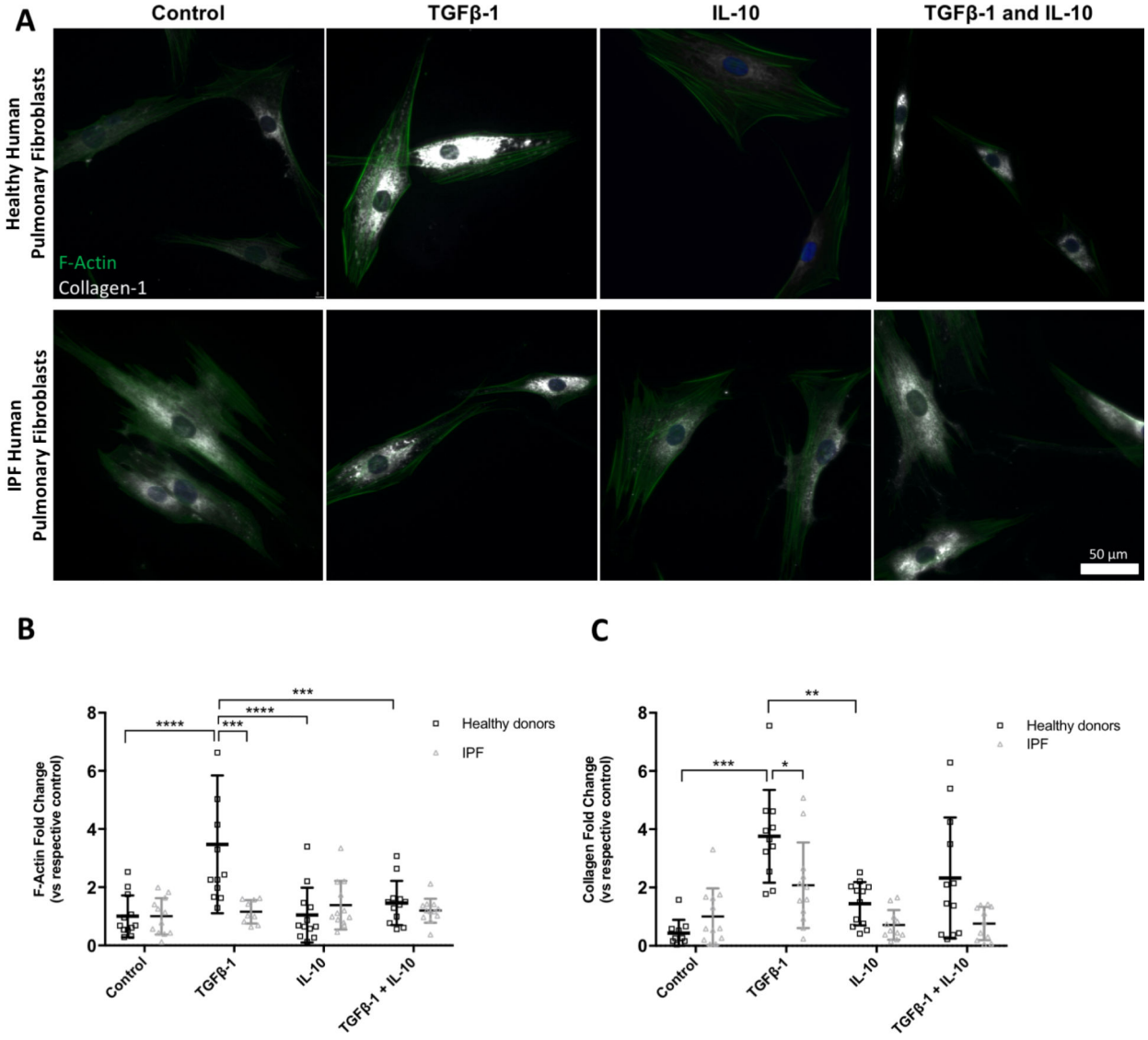

Figure 1. IL-10 mediates TGFβ-1 induced pro-fibrotic stimulus in healthy and IPF lung fibroblasts *in vitro* via attenuated responses to actin stress and collagen deposition

A) Representative immunofluorescence images of healthy (top panels) and IPF (bottom panels) fibroblasts stained for f-actin (green) and collagen-1 (white) under control, TGFβ-1 stimulation (5 ng/mL), IL-10 stimulation (50 ng/mL), or both. B)-C) Quantifications of f-actin (B) and collagen-1 (C) fluorescence images for healthy donor and IPF fibroblasts under noted stimulations at the same concentration as figure 1A. Data is compiled from three separate human cell lines for healthy and IPF fibroblasts; fluorescence was quantified using CTCF and significance was measured and marked. For all graphs- **** p<.0001 *** p< .001; ** p< .01; * p<.05.

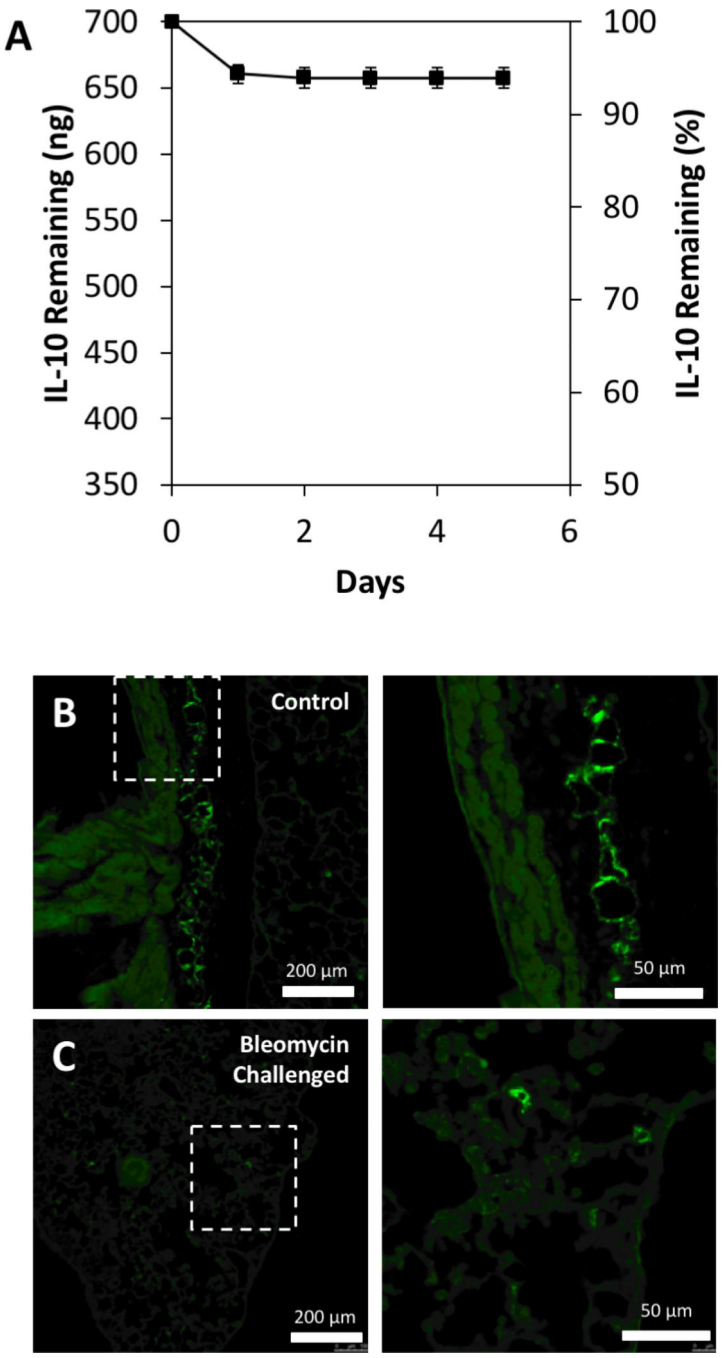

Figure 2. IL-10 immobilization in HH10 and lung deposition of gel.

A) ELISA quantification of IL-10 released from HH-10 formulation over 6 days (n=13). B)-C) Fluorescent microscopy images of lung tissue with fluorescently labeled HH reagent in both healthy (B) and bleomycin-challenged (C) lung tissue, displaying deposition locations of HH reagent via intranasal treatment. Images on right are high magnification of the squared regions.

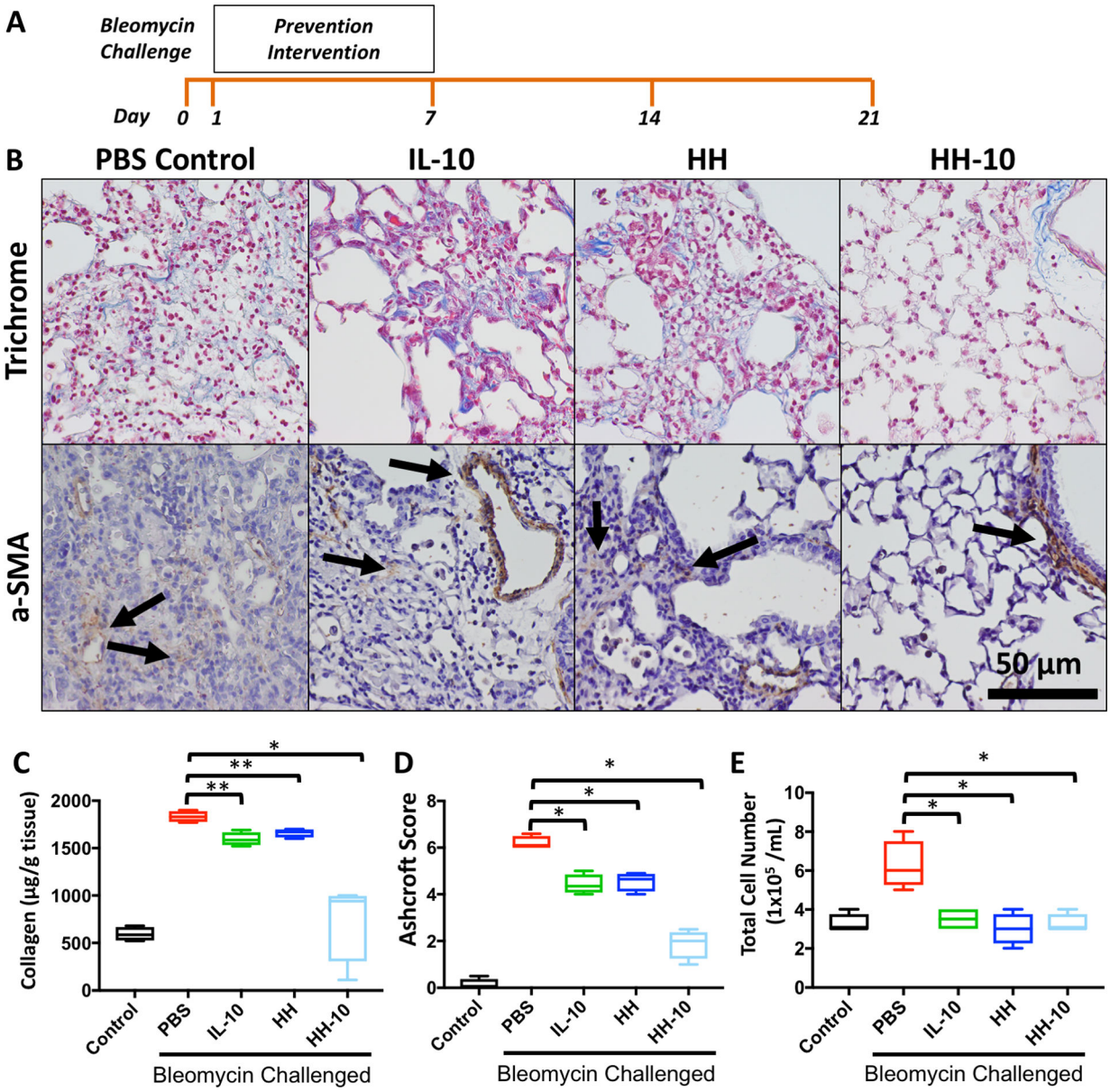

Figure 3. Bleomycin challenged mice show decreased fibrotic and inflammatory character in prevention cohort treated with HH-10.

A) Experimental design timeline of prevention cohort and analysis. B) Trichrome and α-SMA IHC stain of lung tissue sections by group of prevention cohorts, all parameters include bleomycin challenge. C) Sircol- assay quantifying collagen content of lung samples from healthy control and bleomycin challenged mice with preventative PBS, IL-10, HH, or HH-10. D) Ashcroft Score quantifying fibrosis of lung sections from healthy control and bleomycin challenged mice with preventative PBS, IL-10, HH, or HH-10. E) BAL cell counts from healthy control and bleomycin challenged mice with preventative PBS, IL-10, HH, or HH-10. For all graphs- ***p< .001 vs. PBS + BLM, **p< .01 vs. PBS + BLM, *p< . 05 vs. PBS + BLM.

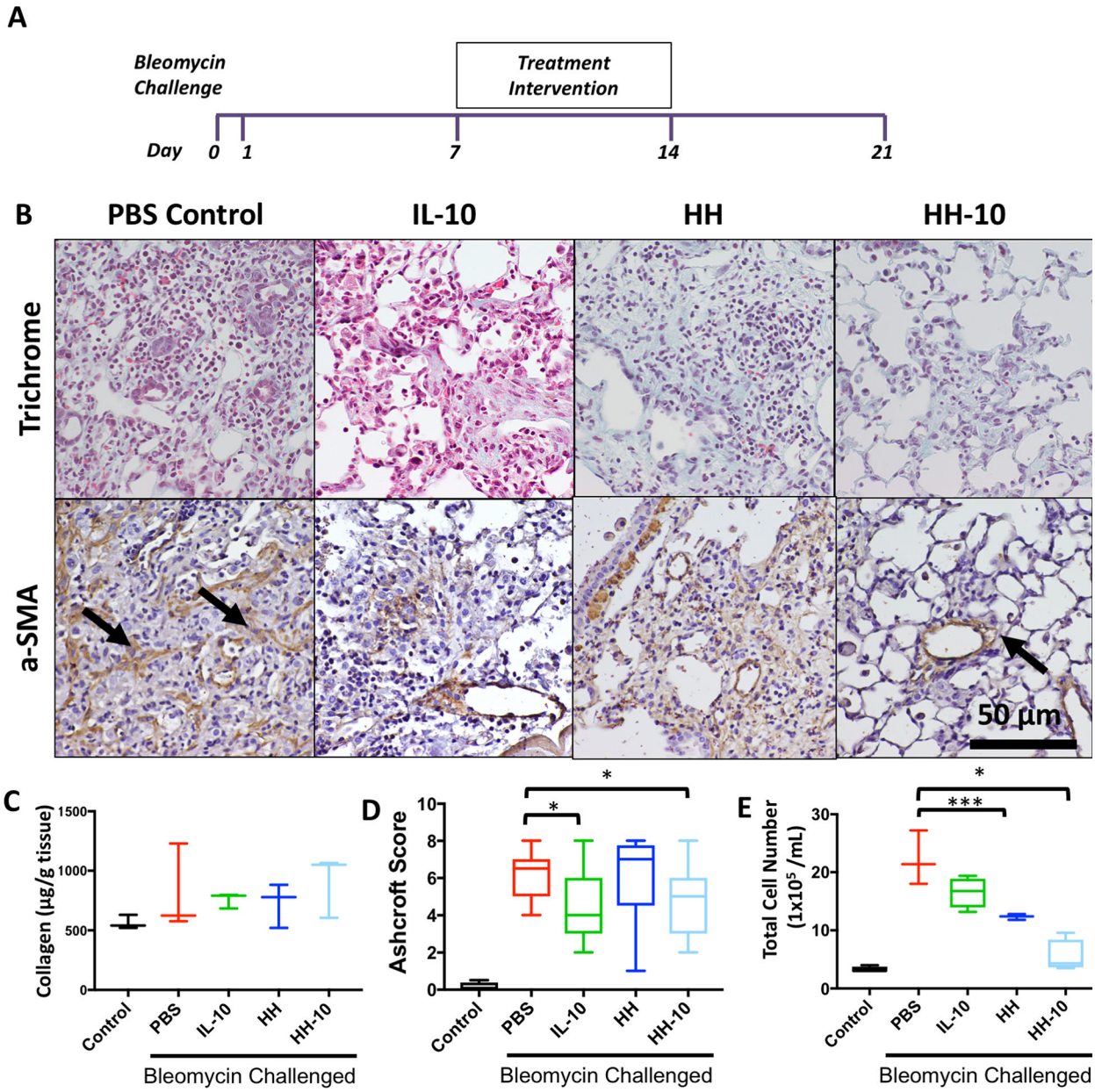

Figure 4. Bleomycin challenged mice show decreased fibrotic and inflammatory character in treatment cohort treated with HH-10.

A) Experimental design timeline of treatment cohort and analysis. B) Trichrome IHC and α-SMA IHC stain of lung tissue sections of bleomycin-challenged treatment cohorts. C) Sircol- assay of lung samples from healthy control and bleomycin challenged mice with PBS, IL-10, HH, or HH-10 treatment. D) Ashcroft Score of lung sections from healthy control and bleomycin challenged mice with PBS, IL-10, HH, or HH-10 treatment. E) BAL cell counts from healthy control and bleomycin challenged mice with PBS, IL-10, HH, or HH-10 treatment. For all graphs- ***p< .001 vs. PBS + BLM, **p< .01 vs. PBS + BLM, *p< .05 vs. PBS + BLM.

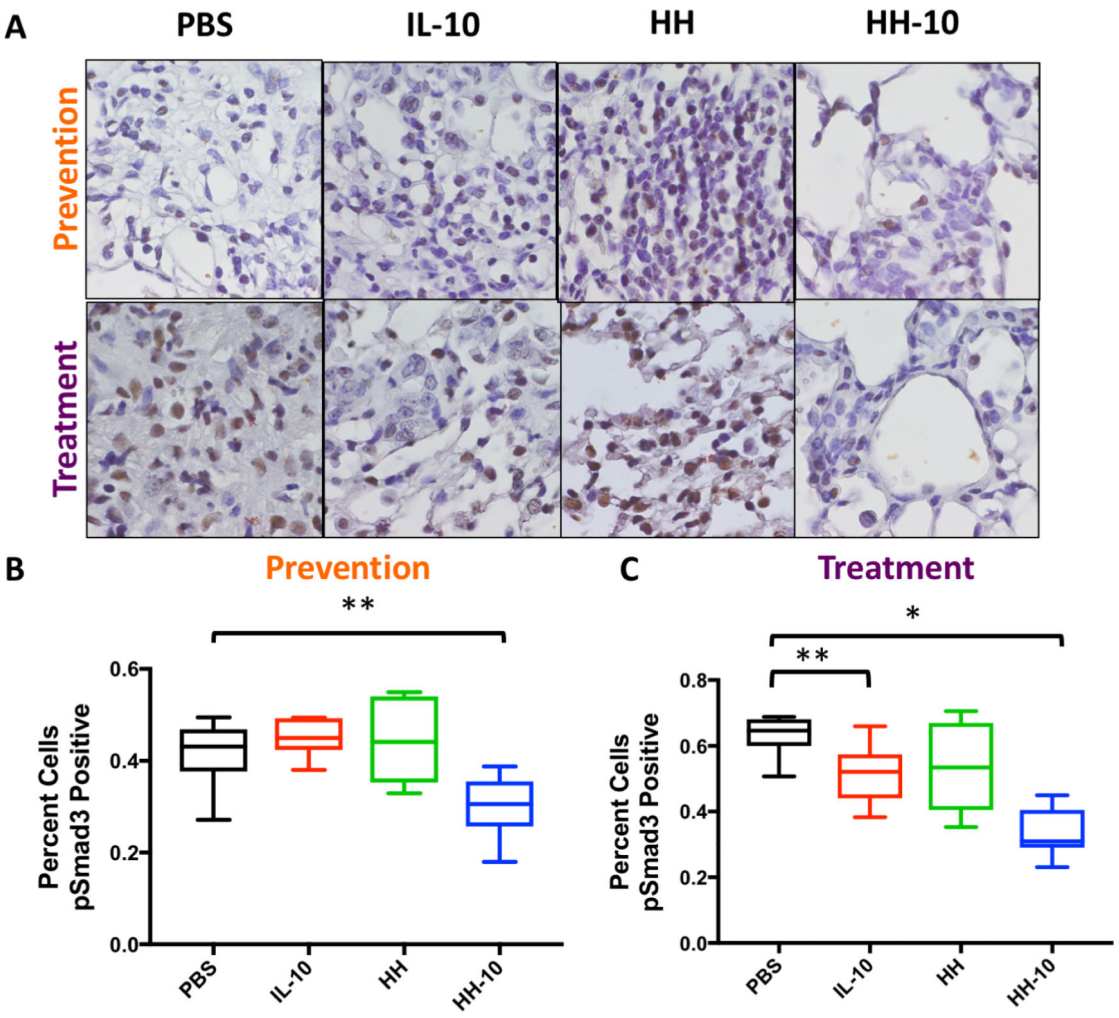

Figure 5. HH-10 treatment reduces Smad3 phosphorylation in both prevention and treatment cohorts.

A) IHC staining for phospho-Smad3 in bleomycin challenged mice treated in prevention or treatment regiments with PBS, IL-10, HH, or HH-10. B)-C) Quantification of pSmad3 positive cells from IHC images in bleomycin challenged mice treated in prevention or treatment regiments with PBS, IL-10, HH, or HH-10. For all graphs- ***p< .001 vs. PBS + BLM and **p< .01 vs. PBS + BLM.